Discrimination of Sleep-Apnea-Related Decreases in the Amplitude Fluctuations of PPG Signal in Children by HRV Analysis

Eduardo Gil*, Martín Mendez, José María Vergara, Sergio Cerutti, *Fellow, IEEE*, Anna Maria Bianchi, *Member, IEEE*, and Pablo Laguna, *Senior Member, IEEE*

***Abstract*—In this paper, an analysis of heart rate variability (HRV) during decreases in the amplitude fluctuations of photopletysmography (PPG) [decreases in the amplitude fluctuations of photopletysmography (DAP)] events for obstructive sleep apnea syndrome (OSAS) screening is presented. Two hundred and sixty-eight selected signal segments around the DAP event were extracted and classified in five groups depending on SaO_2 and respiratory behavior. Four windows around each DAP are defined and temporal evolution of time–frequency HRV parameters was analyzed for OSAS screening. Results show a significant increase in sympathetic activity during DAP events, which is higher in cases associated with apnea. DAP events were classified as apneic or nonapneic using a linear discriminant analysis from the HRV indexes. The ratio of DAP events per hour r_{DAP} and the ratio of apneic DAP events per hour r^a_{DAP} were computed. Results show an accuracy of 79% for r^a_{DAP} (12% increase with respect to r_{DAP}), a sensitivity of 87.5%, and a specificity of 71.4% when classifying 1-h polysomnographic excerpts. As for clinical subject classification, an accuracy of 80% (improvement of 6.7%), a sensitivity of 87.5%, and a specificity of 71.4% are reached. These results suggest that the combination of DAP and HRV could be an improved alternative for sleep apnea screening from PPG with the added benefit of its low cost and simplicity.**

***Index Terms*—Children, decreases in the amplitude fluctuations of photopletysmography (PPG), heart rate variability (HRV), pulse PPG, sleep apnea, time–frequency.**

I. Introduction

OBSTRUCTIVE sleep apnea syndrome (OSAS) is one of the most common sleep pathologies with high prevalence among the general population, with levels reaching values as high as 4% for men, 2% for women, and 3% for children [1]. Generally, sleep apnea goes undiagnosed as painful symptoms do not appear and patients do not seek medical aid. The most common sleep apnea indicators are daytime sleepiness, irritability, tiredness, low concentration, and impaired learning [2]. These factors generally have more serious consequences such as social problems and job and traffic accidents. In addition, OSAS produces hyperactivity and reduced capability to perform mental tasks during childhood [3]. Severe OSAS generates diurnal hypertension and many other potentially fatal cardiovascular effects [4], [5].

OSAS consists of an interruption of the airflow to the lungs produced by an upper airways occlusion. This is accompanied by a decrease of blood oxygen over time and mechanical respiratory efforts that are intensified in order to reopen upper airways. If these efforts are not sufficient and the hypercapnia level is dangerous, an arousal is generated to reactivate all the peripheral systems and respiration is restored. This episode may recur hundreds of times in a single night, with serious health implications [6].

Polysomnography (PSG) is the gold standard procedure for sleep apnea diagnosis. PSG consists of an overnight recording of different electrophysiological signals. The most common signals recorded are electroencephalogram, electromyogram, electrooculogram, electrocardiogram, airflow, and oxygen saturation. The acquisition and analysis of these signals require human experience and specialized equipment. The latter requirements and the reduced number of sleep centers make sleep diagnosis a very expensive procedure. In addition, sleep diagnosis produces a psychological impact in case of child patients [7]–[9].

In the last decade, application of different techniques for home sleep apnea monitoring has been extensively developed [10]. These techniques range from the most sophisticated technology, such as video recording, to simple measures such as photopletysmography (PPG) signal. PPG waveform and its relation with physiological systems have been widely studied for clinical physiological monitoring, vascular evaluation, and autonomic behavior. PPG is an easily acquired measurement and provides a measure of the tissue blood volume, which is related to arterial vasoconstriction or vasodilatation generated by the autonomic nervous system (ANS) and modulated by the heart cycle. Indeed, PPG envelope amplitude decreases as a consequence of vessel constriction generated by the activation of the sympathetic nervous system. Amplitude reduction in PPG

Manuscript received April 23, 2008; revised July 2, 2008. First published November 11, 2008; current version published May 6, 2009. This work was supported in part by the Ministerio de Ciencia y Tecnología, FEDER, under Project TEC2007-68076-C02-02/TCM, by the Heart Cycle Project FP7-216695 of the European Community, and by the Diputación General de Aragón (DGA), Spain, under Grupos Consolidados GTC ref:T30. *Asterisk indicates corresponding author.*

*E. Gil is with the Communications Technology Group, Aragón Institute of Engineering Research (I3A), University of Zaragoza, Zaragoza 50009, Spain, and also with the CIBER de Bioingeniería, Biomateriales y Nanomedicina (CIBER-BBN), Zaragoza 50018, Spain (e-mail: edugilh@unizar.es).

M. Mendez, S. Cerutti, and A. M. Bianchi are with the Department of Biomedical Engineering, Politecnico di Milano, Milano 20133, Italy (e-mail: martin.mendez@biomed.polimi.it; sergio.cerutti@polimi.it; annamaria.bianchi@polimi.it).

J. M. Vergara is with the Sleep Department, Miguel Servet Children Hospital, Zaragoza 50009, Spain, and also with the CIBER de Bioingeniería, Biomateriales y Nanomedicina (CIBER-BBN), Zaragoza 50018, Spain (e-mail: vergeur@comz.org).

P. Laguna is with the Communications Technology Group, Aragón Institute of Engineering Research (I3A), University of Zaragoza, Zaragoza 50009, Spain, and also with the CIBER de Bioingeniería, Biomateriales y Nanomedicina (CIBER-BBN), Zaragoza 50018, Spain (e-mail: laguna@unizar.es).

Digital Object Identifier 10.1109/TBME.2008.2009340

occurs when an apnea event takes place due to sympathovagal balance changes [11], [12].

On the other hand, another electrophysiological signal very broadly studied for apnea diagnosis is heart rate variability (HRV). HRV represents fluctuations in the heart rate related to ANS control. HRV exhibits frequency components from 0 to 0.5 Hz, which could be associated to the ANS branches. The frequency components between 0.15 and 0.5 Hz represent the vagal tone; frequencies in this band are known as high-frequency (HF) components. Frequencies from 0.04 to 0.15 Hz manifest the activation of both parasympathetic and sympathetic nervous systems and these are labeled low-frequency (LF) components. Finally, frequencies between 0.0033 and 0.04 give information of the slow processes such as thermoregulation. Since the relative participation of parasympathetic and sympathetic nervous in the LF component is uncertain, the ratio between HF and LF is defined as the sympathovagal balance [13].

Detection of sleep apnea from PPG [14] and HRV [15]–[18] have been explored independently in the literature. Decrements in the amplitude fluctuations of PPG [decreases in the amplitude fluctuations of photopletysmography (DAP)] events are markers of sympathetic discharge, because sympathetic activity increasingly produces vasoconstriction that is reflected in the PPG signal by decreases in the signal amplitude fluctuation [19], [20]. When apnea occurs, sympathetic activity increases [11], [12]; therefore, DAP events could indirectly quantify apneas during sleep. However, other physiological events such as movements and deep inspiratory gasp produce sympathetic activation, and consequently, decrements in PPG envelope amplitude [21], which are unrelated to apnea. As respiration modulates HR, an HRV analysis could be useful in distinguishing whether DAP events are related to apnea or to other different events. So, the apnea identification by applying detection of decrements in the amplitude fluctuations of PPG DAP as reference point and further spectral parameters analysis of the HRV around this point could offer an integrative procedure that represents an alternative solution to define apnea episodes and obtain more specific apnea screening.

The aim of this study is to analyze the sympathovagal balance during DAPs related and not related to airflow reductions, oxygen desaturations, and no apnea episodes in normal and pathologic children. The dynamics of the sympathovagal balance is obtained by the analysis of spectral parameters of the HRV applying a time–frequency representation called smooth pseudo-Wigner–Ville distribution (SPWVD). Furthermore, a comparison between apnea screening using only PPG and the combination of PPG and HRV is carried out. Section II introduces materials and methods. Section III presents the results that are discussed in Section IV. Finally, Section V gives the conclusions.

II. Materials and Methods

A. Data

One complete night PSG recordings from 21 children were used in this study. Age of the children ranged around 4.47 ± 2.04 years. Children were referred to the Miguel Servet Children's Hospital in Zaragoza for suspected sleep-disordered breathing. EEG with electrode positions C3, C4, O1, and O2, chin electromyogram, ECG with leads I and II, eye movements, airflow, and chest and abdominal respiratory efforts were recorded by a digital polygraph (BITMED EGP800), according to the standard procedure defined by the American Thoracic Society [22]. PPG and arterial oxygen saturation (SaO_2) were measured continuously using a pulse oximeter (COSMO ETCO2/SpO2 Monitor Novametrix, Medical Systems). Signals were stored with a sample rate of 100 Hz, only ECG signals were sampled at 500 Hz. OSAS evaluation from PSG data was scored by clinical experts by using the standard procedures and criteria [1]. Ten children were diagnosed with OSAS and 11 were diagnosed as normal.

B. Decreases in Amplitude Fluctuation of PPG (DAP) Detection

During sleep, apnea or arousal events increase sympathetic tone generating arterial vasoconstriction. Transient sympathetic activations are reflected as DAP [19], [23]. In order to identify DAP events, we applied a detection algorithm based on detecting the envelope reduction of the PPG [14]. A summary of the algorithm steps is presented next. PPG signal $(x_p(n))$ is detrended $(x_{p_{dc}}(n))$ by removing the mean value obtained with a moving average filter. Artifacts were detected in $x_{p_{dc}}(n)$ by an algorithm based on Hjorth parameters, and the artifacted signal segments were rejected. The envelope $x_E(n)$ of $x_{p_{dc}}(n)$ is obtained at the artifact-free signal segments by

$$x_E(n) = \sqrt{\frac{1}{N_p} \sum_{k=n-(N_p-1)}^{n} x_{p_{dc}}^2(k)} \tag{1}$$

where N_p is the number of samples in two cardiac cycles. This was selected according to the results in Gil *et al.* [14]. A DAP event is identified at time n when $x_E(n)$ is lower than a predefined adaptive threshold and this situation has a minimum duration. This adaptive threshold is updated when neither DAP event nor artifacts are present and is calculated as a percentage of the mean of the last L_p nonartifacted samples of the envelope $x_E(n)$.

C. DAP Clustering Criteria Related to Apnea Signs

Medical diagnosis consisted of classifying the available records in the database in two groups: normal or pathologic. DAP events for each recording were detected with the procedure described in Section II-B and [14] at the PPG signal. Segments from ECG, PPG, SaO_2, air flow, and abdominal effort centered at the DAP event onset and lasting 5 min were extracted and from hereon, were denoted as DAP events. From these events, those who had clear signatures were taken to obtain five different groups with uniform patterns based on the gold standard criterion for defining sleep apneas [1]. DAP event is classified into following five groups. Group 1 (G_1) when SaO_2 decreases by at least 3% and there is not a clear reduction in airflow signal. Group 2 (G_2) when airflow decreases by at least 50% with respect to the baseline for a minimum duration of 5 s. Group 3 (G_3) when airflow reduces by more than 50% from baseline and

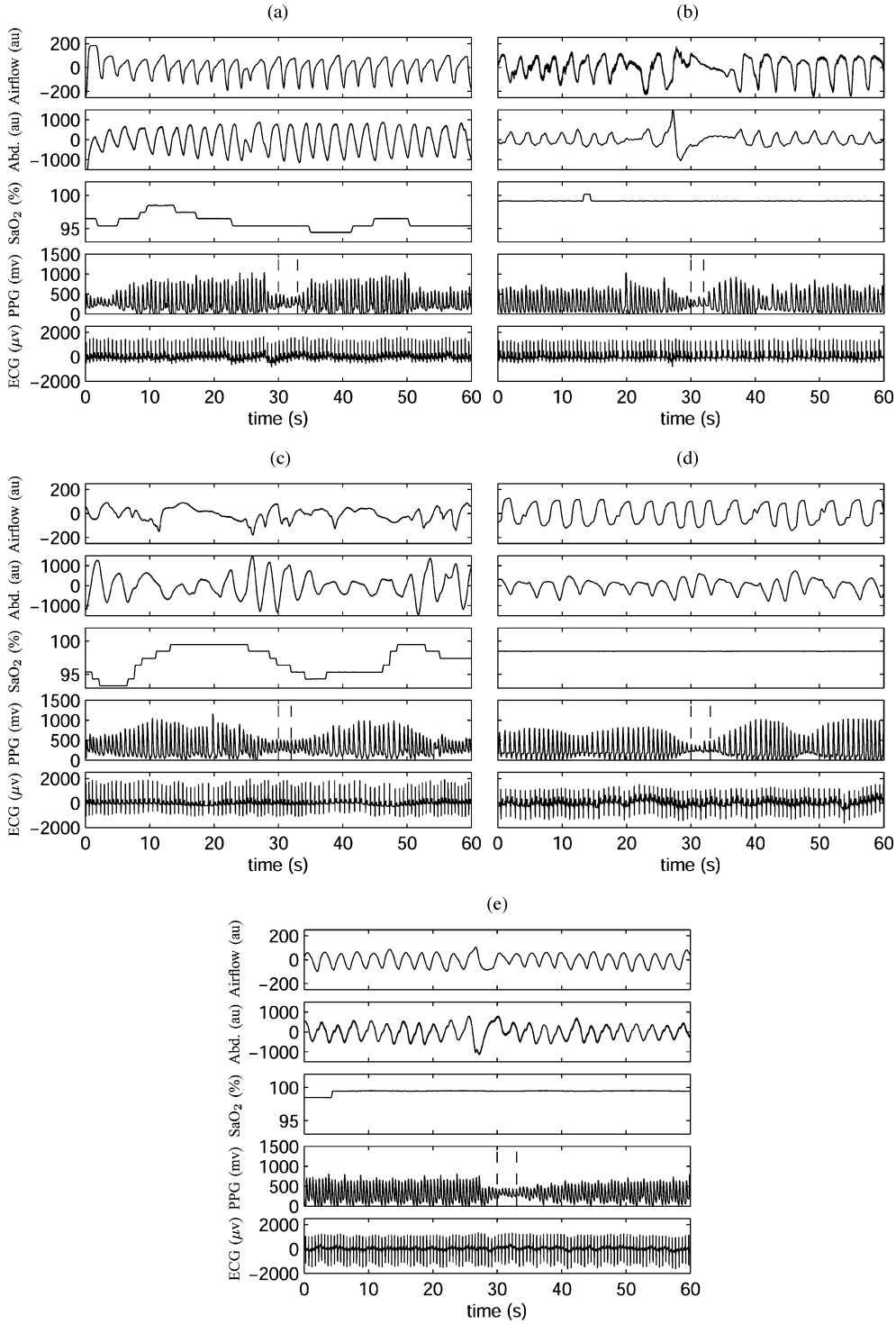

Fig. 1. DAP events examples. The DAP event onset and end (as given by the detector) are marked with dashed lines. (a) G_1. (b) G_2. (c) G_3. (d) G_4. (e) G_5.

is accompanied by a reduction in SaO_2 of at least 3%. Group 4 (G_4) when DAP event correlated neither to airflow reduction nor SaO_2 decrement. Finally, Group 5 (G_5) when DAP events are related neither to apneas nor SaO_2 decrements but a change in respiration occurs. Fig. 1 shows typical examples of airflow, abdominal efforts, SaO_2, PPG, and ECG for the different groups. G_1, G_2, and G_3 can be merged in a single group named G_a (apneic group) as well as G_4 and G_5 can also be regrouped in a single set, G_n (nonapneic group). A total of 268 DAP events were extracted. Table I shows a summary of the DAP events in each group.

Note that G_2 group has a comparable number of events belonging to subjects clinically classified as normal or OSAS, while more could have been expected for OSAS. The reason could be that oxygen desaturation is a leading parameter for clinical diagnosis, so these G_2 events, which do not have a

TABLE I
NUMBER OF DAP EVENTS IN EACH GROUP

Clinical Diagnosis	DAP group					Total
	G_1	G_2	G_3	G_4	G_5	
Normal	4	32	5	76	31	148
OSAS	44	21	33	11	11	120
Total	48	53	38	87	42	268

strong impact on SaO_2, do not necessarily lead to OSAS label explaining this apparent inconsistency.

D. HRV Analysis

Inverse interval function $d_{\mathrm{IIF}}(t_j)$ [24] denoting the heart rate time series was extracted from the ECG segments by an automatic QRS detector [25] providing the t_j beat location for every jth beat. $d_{\mathrm{IIF}}(t_j)$ series were resampled at 2 Hz by cubic spline interpolation. Resulting time series were detrended by subtracting the mean value. Subsequently, analytic signals from each segment were obtained by applying the Hilbert transform to the detrended series. After that, time–frequency representation was used to decompose the signals in their different frequencies at each time. Then, the time evolution of the HRV indexes was evaluated: total power from 0.0033 to 0.5 Hz ($\mathcal{P}_{\mathrm{T}}$), very LF power from 0.0033 to 0.04 Hz ($\mathcal{P}_{\mathrm{VLF}}$), LF power from 0.04 to 0.15 Hz ($\mathcal{P}_{\mathrm{LF}}$), HF power from 0.15 to 0.5 Hz ($\mathcal{P}_{\mathrm{HF}}$), and low to HF ratio ($\mathcal{R}_{\mathrm{LF/HF}}$). The representations and the spectral indexes were obtained by using the absolute values of the time–frequency distributions.

Time–frequency analysis presents interesting mathematical features to analyze short time series with high time–frequency resolution. In our study, a good time resolution is required because apneas in children present rapid changes. Therefore, Cohen's class time–frequency distributions were considered. This class obeys the property of time- and frequency-shift invariance [26]. Cohen's class is defined by

$$C_x(t,f) = \iint \phi(t-t',\tau)x\left(t'-\frac{\tau}{2}\right)x\left(t'+\frac{\tau}{2}\right)e^{-2\pi f\tau}\,dt'\,d\tau \tag{2}$$

where $\phi(t-t',\tau)$ is a function labeled kernel and $x(t)$ is the analytic signal to be analyzed. The kernel properties define the distribution properties. A specific kernel univocally defines a distribution. The kernel is a bidimensions filter, the purpose of which is to eliminate noisy energy components generated by the quadratic nature of the distribution. These spurious components are known as cross terms and disturb the energy signal interpretation in the time–frequency plane. In this study, the kernel used for minimizing the cross-term errors effect was the SPWVD. This distribution was introduced by Martin and Flandrin in 1985 [27] and is characterized by independent smoothing functions in time and frequency, originated by $\varphi(t)$ and $\eta(\tau/2)\eta^*(-\tau/2)$ windows, respectively

$$\phi(t,\tau) = \varphi(t)\eta\left(\frac{\tau}{2}\right)\eta^*\left(-\frac{\tau}{2}\right). \tag{3}$$

The SPWVD parameters were selected in order to allow us to evaluate the spectral components of the HRV with high time and frequency resolution [28], and on the basis of recommendations and experimental results reported in previous studies [29], [30]. For smoothing in time $\varphi(t)$, a Hamming window of 10.5 s was selected, whereas for smoothing in frequency $\eta(\tau/2)$, a Hamming window of 64.5 s was used.

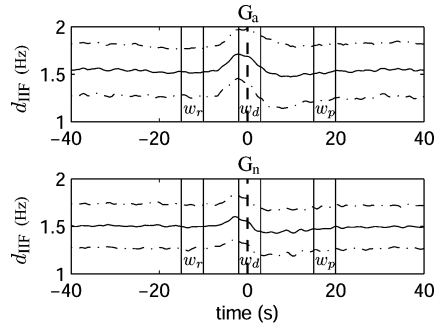

Fig. 2. d_{IIF} mean ± S.D. for apneic ($G_a \equiv G_1+G_2+G_3$) and nonapneic ($G_n \equiv G_4+G_5$) DAP events. Analysis windows (r: reference, d: DAP episode, and p: post DAP event). Dashed line at reference time indicates DAP onset.

E. Statistical Analysis and Classification

1) Statistical Analysis: In order to quantify the evolution of autonomic variations when a DAP event is associated or not associated to airflow decrements, SaO_2 reductions, or to nothing; four time windows were defined in specific time intervals related to DAP events onset. Fig. 2 shows the mean of the d_{IIF} sequences when DAP is related or not related to an apneic episode, as well as the windows defined in relation to DAP event. Time 0 s is assigned to DAP onset. The time windows are defined as follows: 1) reference window (w_r) is located 15 s previous to the DAP event onset with a duration of 5 s; 2) DAP episode window (w_d) is found 2 s before the DAP onset and lasting 5 s; 3) post-DAP event window (w_p) located 15 s after DAP onset and lasting 5 s; and 4) global window (w_g) starting at 20 s prior to the DAP onset, lasting 40 s and containing the other windows. Mean absolute values in the time windows were computed for d_{IIF} sequences, $\mathcal{P}_{\mathrm{VLF}}$, $\mathcal{P}_{\mathrm{LF}}$, $\mathcal{P}_{\mathrm{HF}}$, and $\mathcal{R}_{\mathrm{LF/HF}}$ as well as for the normalized versions with respect to the total power $\mathcal{P}_{\mathrm{VLF}_n}$, $\mathcal{P}_{\mathrm{LF}_n}$, and $\mathcal{P}_{\mathrm{HF}_n}$. Kruskal–Wallis nonparametric statistic approach was performed in two cases: one, to compare the time variations among windows of HRV parameters, and the other, to compare differences among groups for each parameter and window. Posthoc analysis was applied to determine pairs that had statistic differences ($p < 0.05$).

2) Features Sets: From the grouped groups were extracted a series of features in order to select a set of them that could provide separation between normal (apneic-unrelated) and apneic (apneic-related) DAP events. The set of features is formed by the mean and the variance within the four different windows (w_r, w_d, w_p, and w_g) referred to as the DAP detection of d_{IIF}, $\mathcal{P}_{\mathrm{LF}_n}$, $\mathcal{P}_{\mathrm{HF}_n}$, $\mathcal{R}_{\mathrm{LF/HF}}$ indexes. In addition, for each index, the difference between reference w_r and DAP episode window w_d as well as between w_r and post-DAP event window w_p was computed. In order to reduce the biovariability in d_{IIF} temporal indexes, signal was first normalized by subtracting the mean

value and dividing by the variance during the complete (5 min) DAP event. Spectral indexes normalized with respect to the total power were used. Features are denoted as either $\overline{X}_n^w$, $\sigma_{X_n^w}$, or $\Delta\overline{X}_n^{w_1-w_2}$, where the overline and σ denote the mean and variance, respectively, X the main index with $X \in \{d_{\mathrm{IIF}}, \mathcal{P}_{\mathrm{LF}}, \mathcal{P}_{\mathrm{HF}}, \mathcal{R}_{\mathrm{LF/HF}}\}$, the subscript n the normalized version and the superscript w the analysis window (w_r for reference, w_d for DAP episode, w_p for post-DAP event, and g for global), and Δ indicates a differential index and in this case w_1 and w_2 denote the two windows involved. A total of 34 features were extracted.

3) Classifier: A linear discriminant (LD) analysis was used to separate between DAP events related and not related to apnea episodes ($\mathrm{G_a}$ and $\mathrm{G_n}$). Let $\mathbf{y_i} = [y_{1i}, y_{2i}, \ldots, y_{di}]$ be a row vector with d values where each column represents a feature value from ith DAP. And suppose we wish to assign $\mathbf{y_i}$ to class k of the c possible classes, then the discriminant value f_k for each class is evaluated from the following equation:

$$f_k = \boldsymbol{\mu}_k \boldsymbol{\Sigma}^{-1} \mathbf{y}_i^T - \frac{1}{2}\boldsymbol{\mu}_k \boldsymbol{\Sigma}^{-1} \boldsymbol{\mu}_k^T + log(\pi_k) \tag{4}$$

where T represents the transpose and $\boldsymbol{\mu}_k$ is the row mean vector obtained from the whole N_k training vectors belonging to class k. In order to evaluate $\boldsymbol{\mu}_k$, let N be the total number of $\mathbf{y_i}$ in the training set, then $\boldsymbol{\mu}_k$ is obtained by

$$\boldsymbol{\mu}_k = \frac{1}{N_k}\sum_{i=1}^{N_k} \mathbf{y}_{ik}. \tag{5}$$

For a LD classifier, $\boldsymbol{\Sigma}$ represents the pooled covariance and it is evaluated as

$$\boldsymbol{\Sigma} = \frac{1}{N-c}\sum_{k=1}^{c}\sum_{i=1}^{N_k}(\mathbf{y}_{ik} - \boldsymbol{\mu}_k)^T(\mathbf{x}_{ik} - \boldsymbol{\mu}_k). \tag{6}$$

π_k represent the prior probability that y_i belongs to a class k. A practical way to evaluate π_k is

$$\pi_k = \frac{N_k}{N}. \tag{7}$$

Finally $\boldsymbol{y}_i$ is assigned to the class k with higher f_k.

4) Selection and Transformation of the Features: Feature selection can be addressed in different ways, it being possible to evaluate it by statistical analysis of features, wrap methods, principal component analysis, or factor analysis. Wrap methods consist of selecting the features based on the classifier performance by gradually adding one more feature and selecting the combination that provides the highest classification accuracy. The wrap method was used in this paper.

F. Clinical Study

To evaluate the improvement of adding HRV information for OSAS diagnosis based on PPG, a clinical study was carried out. The available one night PSG recordings described in Section II-A were split into 1-h length fragments. These 1-h PSG fragments were labeled as control, doubt, or pathologic based on SaO_2 desaturation in order to later be able to evaluate the classifier accuracy for these fragments. To establish this separation, a baseline level β, corresponding to the SaO_2 signal mode of the entire night recording, was considered [14]. In all recordings $\beta \geq 97\%$. Total time intervals with SaO_2 signal below $\beta - 3\%$, $t_{\beta-3}$ was calculated for each fragment. PSG fragments were classified according to the following criteria:

$$\begin{aligned} t_{\beta-3} &< 0.9\,\mathrm{min} \qquad \text{control} \\ 0.9\,\mathrm{min} < t_{\beta-3} &< 3\,\mathrm{min} \qquad \text{doubt} \\ t_{\beta-3} &> 3\,\mathrm{min} \qquad \text{pathologic.} \end{aligned} \tag{8}$$

This implies a minimum of 5% of the time with evident oxygen desaturation to be considered as pathologic, which corresponds to a severe OSAS criteria in children [31] of 18 apneas per hour having a mean duration of 10 s. For control group, the threshold corresponds to five apneas per hour. Table II shows the classification for these PSG fragments.

TABLE II
PSG FRAGMENTS CLASSIFICATION

Clinical diagnosis	# subjects	# fragments	PSG fragments classification		
			# normal	# doubt	# pathologic
Normal	10	46	42	4	0
Pathologic	11	59	28	20	11
Total	21	105	70	24	11

Now, the objective is to classify these 1-h fragments based on the DAP per hour ratio. This classification will be done both just with the DAP coming from the DAP detector in Section II-B, r_{DAP}, and with those classified as apneic DAP events with the methodology presented in Section II-E, r^a_{DAP}. For training the classifier, DAP events in Section II-C selected from groups $\mathrm{G_1}$–$\mathrm{G_5}$ were used. Receiver operating characteristic (ROC) curves were calculated for both indexes and the optimum thresholds in terms of maximizing sensitivity (Se) and specificity (Sp) were established. In addition, Wilcoxon nonparametric statistical analysis was carried out for both indexes in order to evaluate their discriminant power between groups.

Since we are interested in having a label attached to a patient, we need a rule to determine when a patient with a given number of pathological fragments is considered as a pathologic subject. For that, the percentage of time under pathologic fragments based on r_{DAP} and r^a_{DAP} was analyzed. The threshold for this percentage was selected for maximizing Se and Sp. From the total of 21 children, six subjects were excluded because only less than 4 h had ECG and PPG signals of acceptable quality, so 15 registers were included in this study corresponding to eight OSAS and seven normal according to clinical diagnosis.

III. RESULTS

A. Statistical Analysis Results

Table III shows Kruskal–Wallis analysis results of statistical comparison among groups for each feature. First row is the p-value test. The remaining rows show a number (or numbers) indicating which group (or groups) has statistical differences with the group defining the row.

Fig. 3 shows mean and standard error of $\overline{d}_{\mathrm{IIF}\,n}$, $\sigma_{d_{\mathrm{IIF}\,n}}$, and spectral indexes obtained by SPWVD. Letters refer to the temporal windows analyzed during DAP (r: reference, d: DAP episode,

TABLE III
KRUSKAL–WALLIS ANALYSIS RESULTS OF STATISTICAL COMPARISON AMONG GROUPS FOR EACH FEATURE

	$\sigma_{d_{\mathrm{IIF}_n}}^{w_r}$	$\sigma_{d_{\mathrm{IIF}_n}}^{w_d}$	$\sigma_{d_{\mathrm{IIF}_n}}^{w_p}$	$\sigma_{d_{\mathrm{IIF}_n}}^{w_g}$	$\overline{d}_{\mathrm{IIF}}{}_n^{w_r}$	$\overline{d}_{\mathrm{IIF}}{}_n^{w_d}$	$\overline{d}_{\mathrm{IIF}}{}_n^{w_p}$	$\overline{d}_{\mathrm{IIF}}{}_n^{w_g}$	$\Delta\overline{d}_{\mathrm{IIF}}{}_n^{w_r-w_d}$	$\Delta\overline{d}_{\mathrm{IIF}}{}_n^{w_r-w_p}$
p	0,015	<0,0001	0,085	0,0002	0,194	<0,0001	0,309	0,48	<0,0001	0,435
G_1	-	-	-	-	-	4	-	-	4	-
G_2	-	4 5	-	-	-	4	-	-	4	-
G_3	-	4 5	-	5	-	4	-	-	4	-
G_4	-	2 3	-	5	-	1 2 3 5	-	-	1 2 3	-
G_5	-	2 3	-	3 4	-	4	-	-	-	-

	$\overline{\mathcal{P}}_{\mathrm{LF}_n}^{w_r}$	$\overline{\mathcal{P}}_{\mathrm{LF}_n}^{w_d}$	$\overline{\mathcal{P}}_{\mathrm{LF}_n}^{w_p}$	$\overline{\mathcal{P}}_{\mathrm{LF}_n}^{w_g}$	$\Delta\overline{\mathcal{P}}_{\mathrm{LF}_n}^{w_r-w_d}$	$\Delta\overline{\mathcal{P}}_{\mathrm{LF}_n}^{w_r-w_p}$	$\overline{\mathcal{P}}_{\mathrm{HF}_n}^{w_r}$	$\overline{\mathcal{P}}_{\mathrm{HF}_n}^{w_d}$	$\overline{\mathcal{P}}_{\mathrm{HF}_n}^{w_p}$	$\overline{\mathcal{P}}_{\mathrm{HF}_n}^{w_g}$	$\Delta\overline{\mathcal{P}}_{\mathrm{HF}_n}^{w_r-w_d}$	$\Delta\overline{\mathcal{P}}_{\mathrm{HF}_n}^{w_r-w_p}$
p	0,0039	0,017	0,0047	0,0006	0,297	0,484	<0,0001	<0,0001	<0,0001	<0,0001	0,032	0,218
G_1	-	-	-	-	-	-	4	4	4	4	-	-
G_2	-	-	-	4	-	-	4	4	4 5	4	-	-
G_3	4	4	4	4	-	-	4	4	4 5	4 5	-	-
G_4	3	3	3	2 3	-	-	1 2 3 5	1 2 3 5	1 2 3	1 2 3	-	-
G_5	-	-	-	-	-	-	4	4	2 3	3	-	-

	$\overline{\mathcal{R}}_{\mathrm{LF/HF}}^{w_r}$	$\overline{\mathcal{R}}_{\mathrm{LF/HF}}^{w_d}$	$\overline{\mathcal{R}}_{\mathrm{LF/HF}}^{w_p}$	$\overline{\mathcal{R}}_{\mathrm{LF/HF}}^{w_g}$	$\Delta\overline{\mathcal{R}}_{\mathrm{LF/HF}}^{w_r-w_d}$	$\Delta\overline{\mathcal{R}}_{\mathrm{LF/HF}}^{w_r-w_p}$	$\overline{\mathcal{P}}_{\mathrm{VLF}_n}^{w_r}$	$\overline{\mathcal{P}}_{\mathrm{VLF}_n}^{w_d}$	$\overline{\mathcal{P}}_{\mathrm{VLF}_n}^{w_p}$	$\overline{\mathcal{P}}_{\mathrm{VLF}_n}^{w_g}$	$\Delta\overline{\mathcal{P}}_{\mathrm{VLF}_n}^{w_r-w_d}$	$\Delta\overline{\mathcal{P}}_{\mathrm{VLF}_n}^{w_r-w_p}$
p	<0,0001	<0,0001	<0,0001	<0,0001	<0,0001	0,341	0,0007	<0,0001	<0,0001	<0,0001	0,38	0,668
G_1	4	4	-	4	4	-	4	4	4	4	-	-
G_2	4	4	4	4	4	-	4	4	4	4	-	-
G_3	4	4	4 5	4 5	-	-	4	4	4	4	-	-
G_4	1 2 3 5	1 2 3 5	2 3 5	1 2 3	1 2	-	1 2 3	1 2 3 5	1 2 3	1 2 3	-	-
G_5	4	4	3 4	3	-	-	-	4	-	-	-	-

First row is the p-value test. The remaining rows show a number (or numbers) indicating which group (or groups) has statistical differences with the group associated to the row (first row element).

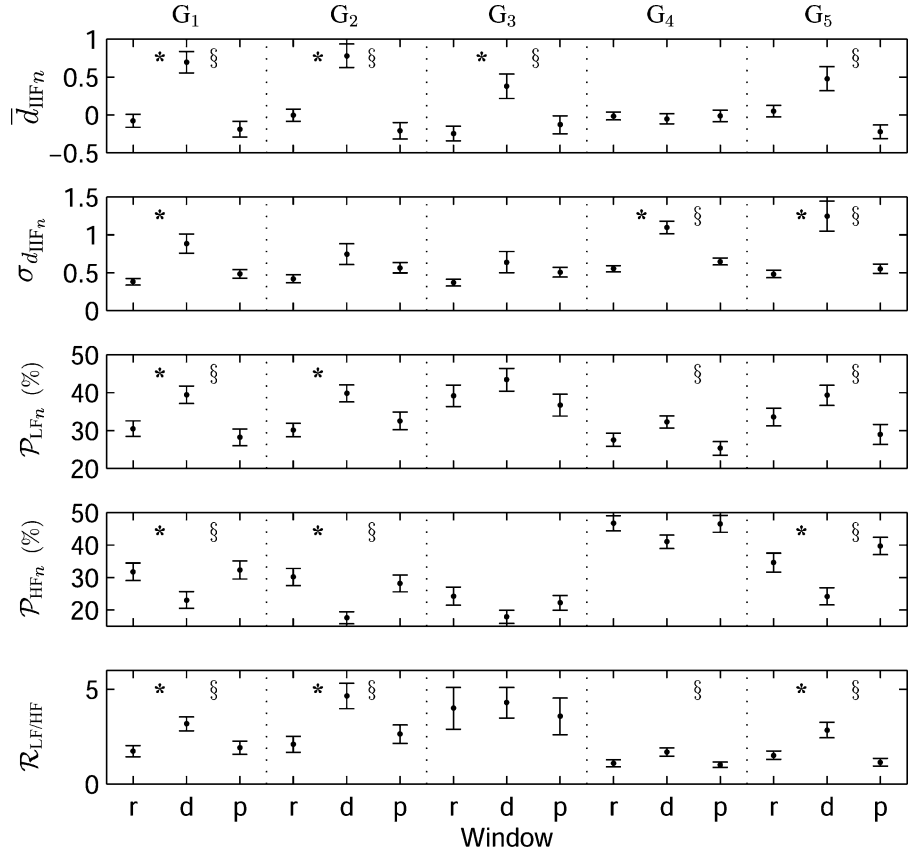

Fig. 3. $\overline{d}_{\mathrm{IIF}\,n} \pm$ SE, $\sigma_{d_{\mathrm{IIF}\,n}} \pm$ SE, and spectral indexes obtained by SPWVD. Window refers to the temporal windows analyzed during DAP (r: reference, d: DAP episode, and p: post DAP event). From top to bottom, mean heart rate ($\overline{d}_{\mathrm{IIF}\,n}$), standard deviation heart rate ($\sigma_{d_{\mathrm{IIF}\,n}}$), LF ($\mathcal{P}_{\mathrm{LF}\,n}$), HF ($\mathcal{P}_{\mathrm{HF}_n}$), and LF to HF ratio ($\mathcal{R}_{\mathrm{LF/HF}}$) of heart rate. All the spectral parameters were normalized with respect to the total power at each time. (*) refers to $p < 0.05$ between windows w_r and w_d and § to $p < 0.05$ between windows w_d and w_p.

TABLE IV
PSG FRAGMENTS CLASSIFICATION RESULTS

Index	PSG Fragments classification			Subjects classification		
	S (%)	S_p (%)	Accuracy (%)	S (%)	S_p (%)	Accuracy (%)
r_{DAP}	81.8	64.3	66.7	75	71.4	73.3
r^a_{DAP}	72.7	80	79	87.5	71.4	80

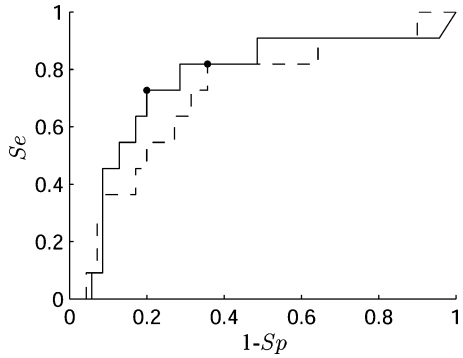

Fig. 4. ROC curves for r_{DAP} (dashed line) and r^a_{DAP} (solid line). Bullet dots indicate the points where the global results are presented.

and p: post DAP event). From top to bottom shown are mean heart rate ($\overline{d}_{\mathrm{IIF}\,n}$), standard deviation heart rate ($\sigma_{d_{\mathrm{IIF}\,n}}$), LF ($\mathcal{P}_{\mathrm{LF}_n}$), HF ($\mathcal{P}_{\mathrm{HF}_n}$), and LF to HF ratio ($\mathcal{R}_{\mathrm{LF/HF}}$) of heart rate. All the spectral parameters were normalized with respect to the total power at each time. (*) refers to $p < 0.05$ between windows w_r and w_d and § to $p < 0.05$ between windows w_d and w_p.

The best features to classify between G_a and G_n obtained by the wrap method were $\overline{\mathcal{P}}^{w_g}_{\mathrm{HF}_n}$, $\overline{\mathcal{R}}^{w_g}_{\mathrm{LF/HF}}$, $\sigma_{d^{w_d}_{\mathrm{IIF}_n}}$, and $\Delta\overline{d}_{\mathrm{IIF}\,n}{}^{w_r-w_d}$, having an accuracy of 68.77%, a $Se = 70.5\%$ and a $Sp = 68.46\%$.

B. Clinical Study Results

Results regarding PSG fragments and subject classification are shown in Table IV. The inclusion of HRV information improves the PSG fragments classification accuracy in 12.3%, reaching a 79%, and obtaining values of 72.7% and 80% for sensitivity and specificity, respectively. In addition, the Wilcoxon statistic analysis shows a higher discriminant power between pathologic and normal for r^a_{DAP} ($p = 0.0061$) than for r_{DAP} ($p = 0.0225$). ROC curves in Fig. 4, varying thresholds in r_{DAP} and r^a_{DAP}, demonstrate the advantage of including HRV information. As for subject classification, the improvement in accuracy is 6.7%, reaching a 80%, and obtaining values of 87.5% and 71.4% for sensitivity and specificity, respectively.

IV. DISCUSSION

Analysis of autonomic control during decreases in the amplitude fluctuation of PPG signal in children was presented. Table III shows statistical differences among G_1, G_2, and G_3 (G_a) with respect to G_4 and G_5 (G_n) for most of the features, confirming the association made in Section II-C based on the apnea physiology. As for time features, $\Delta\overline{d}_{\mathrm{IIF}\,n}{}^{w_r-w_d}$ evidence a higher rise in d_{IIF_n} for DAP associated with apneic events (G_a) than DAP without apnea connection (G_n). Respiration modulates HR, HF being the component that mainly reflects the respiratory process. Our hypothesis is that this modulation is different among groups and at the different temporal windows, these differences being the parameters used to distinguish among groups. Results show that differences (higher $\mathcal{P}_{\mathrm{LF}_n}$ and lower $\mathcal{P}_{\mathrm{HF}_n}$ values) appear in frequency features for all groups with respect to G_4 during all time references (w_r, w_d, w_p, and w_g), indicating a predominance of the sympathetic system during apnea, in agreement with [11], and the fact that different respiratory patterns appear. As $\mathcal{P}_{\mathrm{HF}}$ presents higher values in G_4 and important significant statistical differences with G_a, the feature $\overline{\mathcal{P}}^{w_g}_{\mathrm{HF}_n}$ was the first selected by the wrap method for feature selection (Section II-E4).

Fig. 3 shows increments in d_{IIF} signal during the DAP event window for all groups, except G_4. Time evolution of frequency features shows similar patterns in all groups, an increase in $\mathcal{P}_{\mathrm{LF}_n}$ and $\mathcal{R}_{\mathrm{LF/HF}}$ and a decrease in $\mathcal{P}_{\mathrm{HF}_n}$ during DAP, indicating an activation of the sympathetic branch of the ANS followed by a recovery period. However, increments in the d_{IIF} signal during the DAP event window turn out to be statistically significant with respect to reference and post DAP event window only for groups 1–3. This means that changes are better marked for apneic events as indicated $\Delta\overline{d}_{\mathrm{IIF}\,n}{}^{w_r-w_d}$ in Table II-F. $\mathcal{P}_{\mathrm{LF}_n}$ reveals significant increments only during the DAP event window in G_1 and G_2 with respect to reference window and G_1, G_4, and G_5 with respect to the post DAP event window. DAP event window shows reduction in the $\mathcal{P}_{\mathrm{HF}}$ for all groups; however, significant are found in G_1, G_2, and G_5. $\mathcal{R}_{\mathrm{LF/HF}}$ also presents significances differences in these groups, but with an increment in the DAP event window.

Our main findings were: an increase in sympathetic activity occurs during DAP events in concordance with [19]. When DAP events are not associated to either respiratory events or SaO_2 decrements, HRV shows just a slight alteration and its spectral power is more shifted to the HF component. On the contrary, DAP events associated to apnea produce a stronger variation in the heart rate, and spectral power is concentrated in the LF range. These results suggest that sympathetic activation is deeper in case of association with apnea. The statistical differences between DAP events associated with apnea and those without association indicate that HRV analysis is useful to discriminate between these two groups of events. This has led to better specificity in apnea detection, as corroborated by the clinical study in Section III-B.

PPG signal carries information related to the cardiovascular function as well as blood gases concentration. This signal presents interesting characteristics that can be used to detect apneic episodes. However, its high sensitivity could produce misdetections and overestimate apneic episodes. Generally, in most of the studies, PPG has been directly related with the cardiac function, giving as a result, a measure of the pulse transit time (PTT) [32]–[34]. PTT gives a quantitative measure of the time that a pulse wave needs for passing from one arterial to another, and is evaluated as the time interval between the ECG R peak and the start of the corresponding PPG wave. PTT decreases after an apneic event due to a sympathetic activation related to arousal that produces heart rate increment, higher stroke volume, and

vasoconstriction, which, in turn, generate pulse wave acceleration [35]. However, some other physiological events such as slow-paced breathing [36] and deep inspiratory gasp [37] also induce variation in the PTT that could be mistaken for sympathetic activations. However, this integration loses important information that could be obtained from the heart rate spectral parameters. Heart rate dynamics and spectral parameters offer time and frequency information that discriminates between small cardiovascular variation and more severe ones, as when an apneic episode occurs.

Heart rate control oscillates in a specific range of frequencies. These frequencies characterize ANS control, which is activated or inhibited as a result of feedback mechanisms. Under constant conditions such as rest, autonomic control is very regular and RR sequence shows a stationary pattern. This situation allows the application of techniques such as Fourier transform to obtain the spectral components of the time series. However, under conditions of rapid change such as sit to stand and sleep apnea, autonomic control adapts speedily to satisfy the system requirements, so the RR sequence shows nonstationary behavior. Under such conditions, more sophisticated techniques of signal processing are required to analyze the time evolution of the autonomic control mechanism. Different approaches have been developed to deal with this problem. Time–Frequency [26], Time-Varying [38], and Time-Scale [39] analysis are some of the most powerful tools. In our study, a good time resolution is required because apneas in children present rapid changes. Therefore, Cohen's class time–frequency distributions were considered. For minimizing the cross-term errors effect of these quadratic distributions, the SPWVD was used. The smoothing functions defining the kernel were selected in order to allow us to evaluate the spectral component of HRV with high time and frequency resolution [28].

This methodology could be evolved if the spectral parameters of the heart rate could be extracted from the PPG. In this way, only acquisition of one signal could be enough to analyze sleep apnea episodes. Since PPG signal is a very simple, cheap, and easy to acquire measure, PPG presents great potential for home apnea monitoring, reducing the cost of wearable devices and complex technology for analysis. Processing of PPG signals could be implemented in real time and with a very low computation cost.

Our results fall within the reported interrater reliabilities for sleep scoring [40], where the mean epoch by epoch agreement between five scorers was 73%, and within the interobserver agreement on apnea–hypopnea index (AHI) using portable monitoring of respiratory parameters [41], where the AHI agreement scored by eight physicians was 73% measured by intraclass correlation coefficient.

Many studies have been carried out for OSAS screening attempting to reduce PSG cost and complexity. Different techniques have been proposed, oximetry-based screening being one of the most widely suggested for both the adult and pediatric population. Although these methods have high sensitivity, they tend to have very low specificity [42]. In addition, a confounding factor in children is that obstructive events frequently do not lead to significant oxyhemoglobin desaturation. Pulse oximetry in children has the same limitation as in adults [43]. Brouillette *et al.* [44], in an extensive study involving 349 children, obtained a positive predictive value of 97%, but the negative predictive value was only 53%. Other approaches based on ECG [15] have shown very good results for adults, achieving perfect scores of 100% in accuracy for subjects classification. However, few ECG-based studies are aimed at children, for which physiology is different and important differences in sleep disorders exist [22], [31]. Shouldice *et al.* [45] reported a sensitivity of 85.7% and a specificity of 81.8% in an ECG-based study on children by adapting previous research on adults where information of ECG-derived respiratory signal was included. Cardiorespiratory sleep studies that typically include two or more signals have also been considered. These studies have been shown to be sensitive to OSAS, but mostly in adults [46]. Some other alternatives such as nap studies, clinical history, sonography, or videography exist [43].

In summary, in terms of sensitivity and specificity, the results of our proposed method are similar to [45] or better than [3], [43], [44] currently investigated alternatives for OSAS screening in children. However, performance improvement to reach the accuracy of adult methods would be desirable, and extended studies are needed to corroborate the potential of our method in diagnosing sleep disorders in children.

V. Conclusion

In conclusion, our results suggest that an increase in sympathetic activity occurs during DAP events. When DAP events are not associated to either respiratory events or SaO_2 decrements, HRV shows slight alterations, and its spectral power is more shifted to the HF component. On the contrary, DAP events associated to apnea produce strong variation in heart rate, and spectral power is concentrated in the LF range. These results suggest that sympathetic activation is deeper in case of association with apnea.

The ratio r^a_{DAP} present an increase of 12% in accuracy for classifying 1-h polysomnographic segments with respect to r_{DAP}, reaching 79% and obtaining values of 72.7% and 80% for sensitivity and specificity, respectively. As for subject classification, the improvement in accuracy is 6.7%, reaching 80%, obtaining values of 87.5% and 71.4% for sensitivity and specificity, respectively. Consequently, HRV analysis improves the utility of PPG signal in sleep disorder diagnosis so that the combination of DAP and HRV could be an alternative for sleep apnea screening with the added benefit of low cost and simplicity. Nevertheless, extended studies are needed to corroborate the potential of PPG signal in conjunction with HRV analysis in diagnosing sleep disorders.

References

[1] American Thoracic Society, "Cardiorespiratory sleep studies in children," *Amer. J. Respir. Crit. Care Med.*, vol. 160, pp. 1381–1387, 1999.
[2] D. P. White, "Sleep apnea," *Proc. Amer. Thorac. Soc.*, vol. 3, pp. 124–128, 2006.
[3] American Academy of Pediatrics, "Clinical practice guideline: Diagnosis and management of childhood obstructive sleep apnea syndrome," *Pediatrics,* vol. 109, pp. 704–712, 2002.
[4] T. Young, P. E. Peppard, and D. J. Gottlieb, "Epidemiology of obstructive sleep apnea," *Amer. J. Respir. Crit. Care Med.*, vol. 165, pp. 1217–1239, 2002.

[5] F. J. Nieto, T. B. Young, B. K. Lind, E. Shahar, J. M. Samet, S. Redline, R. B. D'Agostino, A. B. Newman, M. D. Lebowitz, and T. G. Pickering, "Association of sleep-disordered breathing, sleep apnea, and hypertension in a large community-based study," *JAMA*, vol. 283, pp. 1829–1836, 2000.
[6] C. Guilleminault, A. Tilkian, and W. C. Dement, "The sleep apnea syndromes," *Annu. Rev. Med.*, vol. 27, pp. 465–484, 1976.
[7] D. W. Beebe and D. Gozal, "Obstructive sleep apnea and prefrontal cortex: Towards a comprehensive model linking nocturnal upper airway obstruction to daytime cognitive and behavioral deficits," *J. Sleep Res.*, vol. 11, pp. 1–16, 2002.
[8] D. J. Gottlieb, R. M. Vezina, C. Chase, S. M. Lesko, T. C. Heeren, D. E. Weese-Mayer, S. H. Auerbach, and M. J. Corwin, "Symptoms of sleep-disordered breathing in 5-year-old children are associated with sleepiness and problem behaviors," *Pediatrics*, vol. 112, pp. 870–877, 2003.
[9] R. D. Chervin, K. H. Archbold, J. E. Dillon, P. Panahi, K. J. Pituch, R. E. Dahl, and C. Guilleminault, "Inattention, hyperactivity, and symptoms of sleep-disordered breathing," *Pediatrics*, vol. 109, pp. 449–456, 2002.
[10] W. W. Flemons, M. R. Littner, J. A. Rowley, P. Gay, W. M. Anderson, D. W. Hudgel, R. D. McEvoy, and D. I. Loube, "Home diagnosis of sleep apnea: A systematic review of the literature," *Chest*, vol. 124, pp. 1543–1579, 2003.
[11] V. K. Somers, M. E. Dyken, M. P. Clary, and F. M. Abboud, "Sympathetic neural mechanisms in obstructive sleep apnea," *J. Clin. Invest.*, vol. 96, pp. 1897–1904, 1995.
[12] V. A. Imadojemu, K. Gleeson, K. S. Gray, L. I. Sinoway, and U. A. Leuenberger, "Obstructive apnea during sleep is associated with peripheral vasoconstriction," *Amer. J. Respir. Crit. Care Med.*, vol. 165, pp. 61–66, 2002.
[13] A. Malliani, "The pattern of sympathovagal balance explored in the frequency domain," *News Physiol. Sci.*, vol. 14, pp. 111–117, 1999.
[14] E. Gil, J. M. Vergara, and P. Laguna, "Detection of decreases in the amplitude fluctuation of pulse photoplethysmography signal as indication of obstructive sleep apnea syndrome in children," *Biomed. Signal Process. Control*, vol. 3, no. 3, pp. 267–277, Jul. 2008.
[15] T. Penzel, J. McNames, P. de Chazal, B. Raymond, A. Murray, and G. Moody, "Systematic comparison of different algorithms for apnoea detection based on electrocardiogram recordings," *Med. Biol. Eng. Comput.*, vol. 40, no. 4, pp. 402–407, 2002.
[16] K. Dingli, T. Assimakopoulos, P. Wraith, I. Fietze, C. Witt, and N. Douglas, "Spectral oscillations of rr intervals in sleep apnoea/hypopnoea syndrome patients," *Eur. Respir. J.*, vol. 22, pp. 943–950, 2003.
[17] F. Roche, J. M. Gaspoz, I. C. Fortune, P. Minini, V. Pichot, D. Duverney, F. Costes, J. R. Lacour, and J. C. Barthélémy, "Screening of obstructive sleep apnea syndrome by heart rate variability analysis," *Circulation*, vol. 100, no. 13, pp. 1411–1415, 1999.
[18] F. Roche, V. Pichot, E. Sforza, I. Court-Fortune, D. Duverney, F. Costes, M. Garet, and J. C. Barthélémy, "Predicting sleep apnoea syndrome from heart period: A time–frequency wavelet analysis," *Eur. Respir. J.*, vol. 22, pp. 937–942, 2003.
[19] M. Nitzan, A. Babchenko, B. Khanokh, and D. Landau, "The variability of the photoplethysmographic signal—A potential method for the evaluation of the autonomic nervous system," *Physiol. Meas.*, vol. 19, pp. 93–102, 1998.
[20] R. P. Schnall, A. Shlitner, J. Sheffy, R. Kedar, and P. Lavie, "Periodic, profound peripheral vasoconstriction—A new marker of obstructive sleep apnea," *Sleep*, vol. 22, no. 7, pp. 939–946, 1999.
[21] J. Allen, "Photoplethysmography and its application in clinical physiological measurement," *Physiol. Meas.*, vol. 28, no. 3, pp. R1–R39, 2007.
[22] American Thoracic Society, "Standards and indications for cardiopulmonary sleep studies in children," *Amer. J. Respir. Crit. Care Med.*, vol. 153, pp. 866–878, 1996.
[23] Y. Mendelson, "Pulse oximetry: Theory and applications for noninvasive monitoring," *Clin. Chem.*, vol. 38, no. 9, pp. 1601–1607, 1992.
[24] L. Sörnmo and P. Laguna, *Bioelectrical Signal Processing in Cardiac and Neurological Applications*. New York: Academic/Elsevier, 2005.
[25] J. P. Martinez, R. Almeida, S. Olmos, A. P. Rocha, and P. Laguna, "A wavelet-based ECG delineator: Evaluation on standard databases," *IEEE Trans. Biomed. Eng.*, vol. 51, no. 4, pp. 570–581, Apr. 2004.
[26] L. Cohen, "Time–frequency distributions—A review," *Proc. IEEE*, vol. 77, no. 7, pp. 941–981, Jul. 1989.
[27] W. Martin and P. Flandrin, "Wigner-ville spectral analysis of nonstationary processes," *Acoust., Speech, Signal Process.*, vol. 33, pp. 1461–1470, 1985.
[28] M. O. Mendez, A. M. Bianchi, N. Montano, V. Patruno, E. Gil, C. Mantaras, S. Aiolfi, and S. Cerutti, "On arousal from sleep: Time–frequency analysis," *Med. Biol. Eng. Comput.*, vol. 46, no. 4, pp. 341–351, 2008.
[29] S. Pola, A. Macerata, M. Emdin, and C. Marchesi, "Estimation of the power spectral density in nonstationary cardiovascular time series: Assessing the role of the time–frequency representations (tfr)," *IEEE Trans. Biomed. Eng.*, vol. 43, no. 1, pp. 46–59, Jan. 1996.
[30] L. T. Mainardi, A. M. Bianchi, and S. Cerutti, "Time–frequency and time-varying analysis for assessing the dynamic response of cardiovascular control," *Crit. Rev. Biomed. Eng.*, vol. 30, pp. 175–217, 2000.
[31] C. L. Marcus, "Sleep-disordered breathing in children," *Amer. J. Respir. Crit. Care Med.*, vol. 164, pp. 16–30, 2001.
[32] D. Pitson, N. Chhina, S. Knijn, M. van Herwaaden, and J. Stradling, "Changes in pulse transit time and pulse rate as markers of arousal from sleep in normal subjects," *Clin. Sci. (Lond.)*, vol. 87, pp. 269–273, 1994.
[33] J. E. Naschitz, S. Bezobchuk, R. Mussafia-Priselac, S. Sundick, D. Dreyfuss, I. Khorshidi, A. Karidis, H. Manor, M. Nagar, E. R. Peck, S. Peck, S. Storch, I. Rosner, and L. Gaitini, "Pulse transit time by r-wave-gate infrared photoplethysmography: Review of the literature and personal experience," *J. Clin. Monit. Comput.*, vol. 18, pp. 333–342, 2004.
[34] D. Pitson, A. Sandell, R. van den Hout, and J. Stradling, "Use of the pulse time as a measure of inspiratoy effort in patients with obstructive sleep apnea," *Eur. Respir. J.*, vol. 8, pp. 1669–1674, 1995.
[35] J. L. Pépin, N. Delavie, I. Pin, C. Deschaux, J. Argod, M. Bost, and P. Levy, "Pulse transit time improves detection of sleep respiratory events and microarousals in children," *Chest*, vol. 127, pp. 722–730, 2005.
[36] M. J. Drinnan, J. Allen, and A. Murray, "Relation between heart rate and pulse transit time during paced respiration," *Physiol. Meas.*, vol. 22, pp. 425–432, 2001.
[37] J. Allen and A. Murray, "Age-related changes in peripheral pulse timing characteristics at the ears, thumbs and toes," *J. Hum. Hypertens.*, vol. 16, pp. 711–717, 2002.
[38] A. M. Bianchi, L. T. Mainardi, E. Petrucci, M. G. Signorini, and S. Cerutti, "Time-variant power spectrum analysis for the detection of transient episodes in HVR signal," *IEEE Trans. Biomed. Eng.*, vol. 40, no. 2, pp. 136–144, Feb. 1993.
[39] S. Mallat, *A Wavelet Tour of Signal Processing*, 2nd ed. New York: Academic, 1999.
[40] R. G. Norman, I. Pal, C. Stewart, J. A. Walsleben, and M. D. Rapoport, "Interobserver agreement among sleep scorers from different centers in a large dataset," *Sleep*, vol. 23, pp. 901–908, 2000.
[41] P. O. Bridevauxa, J. W. Fittinga, J. M. Fellratha, and J. D. Auberta, "Inter-observer agreement on apnoea hypopnoea index using portable monitoring of respiratory parameters," *Swiss Med. Weekly*, vol. 137, pp. 602–607, 2008.
[42] Standards of Practice Committee American Sleep Disorders Association, "Portable recording in the assessment of obstructive sleep apnea," *Sleep*, vol. 17, no. 4, pp. 378–392, 1994.
[43] M. S. Schechter, "Technical report: Diagnosis and management of childhood obstructive sleep apnea syndrome," *Pediatrics*, vol. 109, no. 4, pp. e69–e69, Apr. 2002.
[44] R. T. Brouillette, A. Morielli, A. Leimanis, K. A. Waters, R. Luciano, and F. M. Ducharme, "Nocturnal pulse oximetry as an abbreviated testing modality for pediatric obstructive sleep apnea," *Pediatrics*, vol. 105, pp. 405–412, 2000.
[45] R. B. Shouldice, L. M. O'Brien, C. O'Brien, P. Chazal, D. Gozal, and C. Heneghan, "Detection of obstructive sleep apnea in pediatric subjects using surface lead electrocardiogram features," *Sleep*, vol. 27, no. 4, pp. 784–791, 2004.
[46] G. M. Nixon and R. T. Brouillette, "Diagnostic techniques for obstructive sleep apnoea: Is polysomnography necessary?," *Paediatr. Respir. Rev.*, vol. 3, pp. 18–24, 2002.

Eduardo Gil was born in Zaragoza, Spain, in 1978. He received the M.S. degree in telecommunication engineering from the University of Zaragoza (UZ), Zaragoza, in 2002, and the Master's degree "Master Universitario en Sueño: Fisiología y Medicina" from the University Pablo Olavide of Sevilla, Sevilla, Spain, in 2007. He is currently working toward the Ph.D. degree at the Department of Electronic Engineering and Communications, UZ.

Since 2006, he has been an Assistant Professor in the Department of Electronic Engineering and Communications, UZ. His current research interests include the field of biomedical signal processing, espacially in the analysis of the photopletismography signal of obstructive sleep apnea diagnosis.

Martín Mendez received the Engineer degree in electronics from the Tecnologico de Aguascalientes, Aguascalientes, Mexico, in 2001, the M.Sc. degree in bioengineering from the Universidad Autonama Metropolitana, México, in 2003, and the Ph.D. degree from the Department of Bioengineering, Politecnico di Milano, Milano, Italy, in 2007.

He is currently with the Department of Bioengineering, Politecnico di Milano, where he is engaged in the analysis and classification of bioelectrical signals during sleep and related pathologies (such as sleep apnea) using parametric and nonparametric approaches as well as pattern recognition techniques.

José María Vergara was born in Vitoria, Spain, in 1952. He received the M.D. and Ph.D. degrees from the University of Zaragoza, Zaragoza, Spain, in 1977 and 1990, respectively.

Since 1981, he has been a Clinical Neurophysiologist at the Miguel Servet Children's Hospital, Zaragoza. He is currently an Associate Professor at the University of Zaragoza. His current research interests include the field of sleep and q-EEG.

Sergio Cerutti (M'81–SM'97–F'03) is currently a Professor in biomedical signal and data processing in the Department of Biomedical Engineering, Politecnico di Milano, Milano, Italy, where he was the Chairman from 2000 to 2006. His current research interests include the following topics: biomedical signal processing (ECG, blood pressure signal and respiration, cardiovascular variability signals, EEG, and evoked potentials), cardiovascular modeling, neurosciences, and regulation and standards in medical equipments and devices. Since 1983, he has been going through a course at a graduate level biomedical signal processing at Engineering Faculties (Milan and Rome) as well as at the Specialisation Schools of Medical Faculties (Milan and Rome). He has authored or coauthored more than 400 international scientific contributions (more than 160 on indexed scientific journals).

Prof. Cerutti was a Member of the IEEE Engineering in Medicine and Biology Society (EMBS) AdCom (Region 8) from 1993 to 1996. He is a Fellow Member of the European Alliance for Medical and Biological Engineering and Science (EAMBES) and an Associate Editor of the IEEE TRANSACTIONS ON BIOMEDICAL ENGINEERING. He is a member of the Steering Committee of the IEEE-EMBS Summer School on Biomedical Signal Processing. He was the Local Organizer of four Summer Schools held in Siena, Italy.

Anna Maria Bianchi (M'93) received the Laurea degree from the Politecnico di Milano, Milano, in 1987.

From 1987 to 2000, she was a Research Assistant in the Laboratory of Biomedical Engineering, Istituto di Ricovero e Cura a Carattere Scientifico (IRCCS) S. Raffaele Hospital, Milano, where she was engaged research in connection with the Department of Biomedical Engineering, Polytechnic University. Since 2001, she has been a Research Assistant in the Department of the Biomedical Engineering, Politecnico di Milano, where she is also an Assistant Professor of fundamentals of electronic bioengineering in the Biomedical Engineering School and of biomedical signal and data processing in the Ph.D. course, and since 2004, she has been on the board of the Ph.D. Program in bioengineering. She has authored or coauthored about 50 peer-reviewed international papers. She is the Local Coordinator of a national Ministero dell'lUniversitá e della Ricerca (MIUR) Project and an European IP Project in the area of biomedical signal processing.

Dr. Bianchi is a member of the IEEE Engineering in Medicine and biology Society and a reviewer of many international journals on Biomedical Engineering.

Pablo Laguna (M'92–SM'06) was born in Jaca, Spain, in 1962. He received the M.S. and Ph.D. degrees in physic science from the Science Faculty, University of Zaragoza, Zaragoza, Spain, in 1985 and 1990, respectively.

From 1987 to 1992, he was an Assistant Professor of automatic control in the Department of Control Engineering, Politecnic University of Catalonia (UPC), Barcelona, Spain and a Researcher in the Biomedical Engineering Division, Institute of Cybernetics (UPC–CSIC). From 1992 to 2005, he was an Associate Professor at the University of Zaragoza, where he is currently a Full Professor of signal processing and communications in the Department of Electrical Engineering, Engineering School, and a Researcher at Aragón Institute for Engineering Research (I3A). Together with L. Sörnmo, he is the author of *Bioelectrical Signal Processing in Cardiac and Neurological Applications* (Elsevier, 2005). His current research interests include signal processing, in particular, applied to biomedical applications.